CHARACTERISTICS AND DURABILITY OF ALKALI ACTIVATED SLAG-MICROSILICA PASTES SUBJECTED TO SULPHATE AND CHLORIDE IONS ATTACK

[#]MOHAMED HEIKAL*, **, SAHAR M. IBRAHIM*

*Chemistry Department, Faculty of Science, Benha University, Benha, Egypt,
**Chemistry Department, College of Science, Al Imam Mohammad Ibn Saud Islamic University (IMSIU),
P.O Box 90950 Riyadh 11623, Saudi Arabia

[#]E-mail: ayaheikal@hotmail.com

Submitted November 23, 2014; accepted April 27, 2015

Keywords: Alkaline activation, Mechanical properties, Electrical conductivity, Thermogravimetric analysis (TGA), Electron microscopy (SEM)

This research aims to produce cementless eco-friendly binding material using alkaline activation of blast-furnace slag (GBFS) and microsilica (MS). The preparation of cementless binding material was conducted with different GBFS-MS mass ratios (100:0; 98:2; 96:4; 92:8) with 0.75:0.50; Na_2O:SiO_2 mol kg^{-1} of GBFS-MS. The characteristics and durability of alkali activated GBFS and MS mixes were studied. Chemically combined water, combined slag contents as well as compressive strength increase with MS up to 4 mass %, then decreases with MS up to 8 mass %. Increase of MS content up to 8 mass %, the compressive strength shows a lower values at early ages (3-14 days). But, at later age up to 28-90 days, the compressive strength values increase. SEM micrographs show the presence of C–S–H and (N,C)–A–S–H gel with low porosity. The alkali activated GBFS-MS pastes are more durable in 5 % $MgSO_4$ or 5 % $MgCl_2$ solution than ordinary Portland cement (OPC) up to 180 days.

INTRODUCTION

The cement industry is non eco-friendly environmental industry due to the continuous emission of CO_2 during the formation of clinker and quarrying operation of raw materials (limestone and clay) accompanying the fabrication process. A binder can be obtained by the reaction of industrial by-products such as blast-furnace slag (GBFS) and microsilica with the alkali activated solution. Alkali activated eco-friendly binder depends on the nature of the raw materials, different reaction products are developed having different microstructures. The reaction product obtained is an inorganic polymer of amorphous nature formed by hydrated aluminosilicate chains 'geopolymer' [1].

GBFS is a by-product of the manufacturing of iron in a blast-furnace where iron ore, limestone and coke are heated up to 1500°C. Two products are produced–molten iron and molten slag. The molten slag is lighter, floats on the top of the molten iron. This molten slag comprises mostly silicates and alumina, combined with some oxides from the limestone. Rapid quenching slag forms granular particles, prevents the formation of crystal lattices. The resulting granular material comprises non-crystalline calcium-aluminosilicates [2].

Microsilica is a by-product of the manufacture of silicon and ferro-silicon alloys by reducing quartz to silicon in an induction arc furnace at 2000°C. Gasified SiO_2 at high temperatures condenses in the low-temperature zone to tiny spherical particles consisting of non-crystalline silica. The chemical composition of MS depends not only upon the raw materials used, but also upon the quality of electrodes and the purity of silicon product [3]. MS particle has an average diameter in the order of 0.1 μm, and its surface areas in the range 2000 - 2500 $m^2 \cdot kg^{-1}$. Because of its small particles size and highly reactivity, MS is often used as a component of densely packed cementing materials, including alkali-activated cements, with high strength and low permeability [4].

Although the literature has numerous articles on alkali-activated pastes as shown [5-9]. Mechanism of alkali-activated aluminosilicates containing a calcium bearing compound differs from the geopolymeric reaction. The type of calcium bearing compound plays an important role in the alkali activation aluminosilicate materials. Alkalis attack aluminosilicate solid waste particles break the outer layer, and then a polycondensation of reaction products take place [5]. Solid state mechanism dominates by slow diffusion of the

ionic species of the unreacted core at later stages. Alkali activated cation (M^+) acts as a catalyst and structure creators for the reaction in the initial stages of hydration, via cation exchange with the Ca^{2+} ions [6, 7]. The nature of the anion in the solution also plays a determining role in activation, particularly in early ages and especially with regard to paste setting [8, 9]. The final products of the GBFS reaction are similar to the products of cement hydration (C–S–H); the major difference being the rate and intensity of the reaction.

This paper represents experimental trials of alkali activated GBFS-MS to produce cementless binding material. This study aims to provide solutions for: lower emission of pollutants into atmosphere by replacing OPC system with alkali activated binders, reduction in consumption of natural resources required in OPC manufacture, reduction in the amount of fuel required in OPC manufacture and eliminating the problems related with GBFS and MS disposals. However, this study will therefore add valuable knowledge to the durability of alkali activation binders. The current study also, aims to investigate physico-chemical and mechanical characteristics of alkali activation binders on electrical conductivity, compressive strength, bulk density, and porosity as well as chemically combined water and combined slag contents when GBFS was partially replaced with MS at levels up to 8 mass %, which activated with a combination of sodium silicate and sodium hydroxide.

EXPERIMENTAL

Blast-furnace slag (GBFS) was provided from Iron and Steel Company, Helwan Governorate, Egypt. The XRD pattern indicates that GBFS is an amorphous material, a broad diffuse hump peak in the region of 20 - 38° 2θ was observed. Blaine surface area of GBFS was ≈ 450 $m^2 \cdot kg^{-1}$. GBFS is composed of angular particles of varying sizes [10]. The chemical analysis of GBFS was given in Table 1.

Table 1. Chemical composition of starting materials, mass %.

Oxide composition (%)	GBFS	MS	OPC	SSL
SiO_2	37.81	94.82	20.41	30.7
Al_2O_3	13.14	0.55	4.94	–
Fe_2O_3	0.23	2.12	3.4	–
CaO	38.70	0.00	63	–
MgO	7.11	0.0	1.9	–
SO_3	1.19	0.7	3.02	–
Na_2O	1.03	0.2	0.4	10.3
K_2O	0.19	0.05	0.22	–
TiO_2	0.34	–	–	–
P_2O_5	0.16	–	–	–
L.O.I	0.00	1.20	2.74	59.0
Total	99.90	99.95	100.03	100.0

Micro-silica (MS) is a by-product of ferrosilicon industries, Aswan, Egypt. The average particles diameter of MS was ≅ 0.1 μm. The chemical analysis is given in Table 1. XRD patterns, FT-IR spectra and FE-SEM are shown in Figures 1-3. MS is completely amorphous. FT-IR spectra of MS show the stronger absorbance bands at 1119.71; 807.78 and 480.61 cm^{-1} (Figure 2). The broad band centered at 1119.71 cm^{-1} is attributed to asymmetric stretching frequency of Si–O–Si, the band centered at 807.78 cm^{-1} is due to symmetric stretching of Si–O–Si, and the band at 480.61 cm^{-1} is due to the bending frequency of O–Si–O. MS particles are densely packed with sphere like particles, and individual particles as shown in Figure 3 [11]. Blaine surface area of MS is 2090 $m^2 \cdot kg^{-1}$.

Sodium silicate liquid (SSL) was provided from Islamic Silicate Industry, Badr City, Helwan. Sodium silicate liquid contains 30.7 % SiO_2, 10.3 % Na_2O and 59 % H_2O, its silica modulus SiO_2/Na_2O equal 2.98 and density of 1440 $kg \cdot m^{-3}$. NaOH was produced by SHIDO Company with purity 99 %.

The ingredients of prepared mixes were blended in a porcelain ball mill to ensure complete homogeneity. Mix compositions were prepared as shown in Table 2. The mixing process was performed according to ASTM

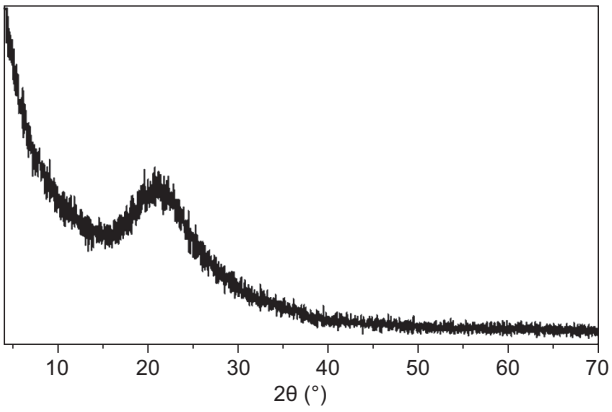

Figure 1. XRD pattern of MS.

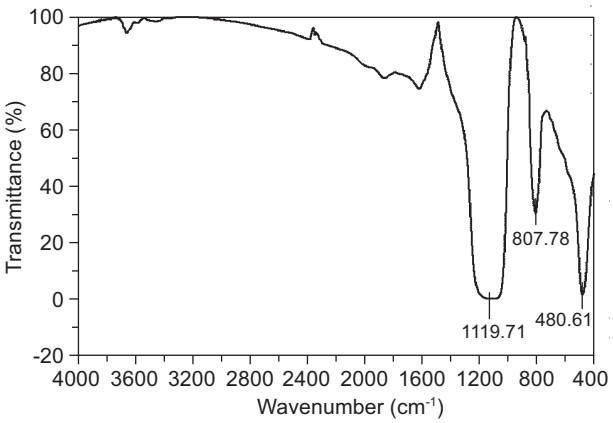

Figure 2. Figure 2: FT-IR spectra of MS.

specification [12]. The pastes were moulded in one inch cubic moulds. Specimens were cured in 100 % RH at 40°C for 24 h. After moulding specimens were cured in the humidifier cabinet up to 3 days, and then cured under tap water at 28°C up to 90 days. Specimens subjected to the resistivity against 5 % magnesium sulphate and 5 % magnesium chloride as aggressive attack solutions were cured up to 7 days (zero time) in tap water then immersed in 5 % $MgSO_4$ or $MgCl_2$ aggressive solution up to 180 days. The aggressive solution was renewed after two weeks to maintain constant concentration of aggressive solution.

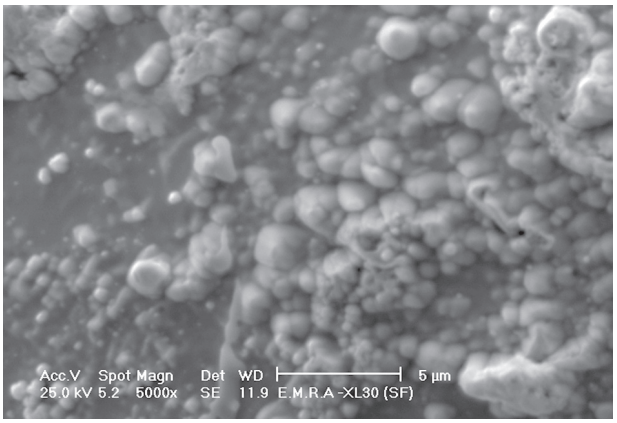

Figure 3. SEM of MS.

Table 2. Composition of the investigated mixes containing alkaline activator (SiO_2 + Na_2O).

Mix No.	GBFS	MS	SiO_2 (mol·kg^{-1} of GBFS+MS)	Na_2O (mol·kg^{-1} of GBFS+MS)	H_2O (ml·kg^{-1} of GBFS+MS)
M0	100	0	0.50	0.75	300
M1	98	2	0.50	0.75	300
M2	96	4	0.50	0.75	300
M3	92	8	0.50	0.75	300
OPC	–	–	–	–	300

Electrical conductivity was measured according to publications [10, 13, 14]. The electrodes were connected with RLC meter, model SR-720, at relativity low AC frequency (1000 Hz) and 1 V for resistance measurements. The mixing of the pastes was done with 300 ml kg^{-1} of GBFS+MS in the presence of alkaline activator (0.50/0.75; SiO_2/Na_2O mol kg^{-1} of GBFS+MS). The pastes were placed in the space between the electrodes [10, 13, 14]. The cell was kept in 100 % relative humidity cabinet chamber during the electrical conductivity measurements test period up to 28 days.

The bulk density and total porosity was conducted, before the pastes subjected to compressive strength determination [15]. After, the determination of bulk density, four cubes of the same age where used for compressive strength testing according to ASTM Specifications (ASTM Designation: C-150, 2007). The hydration of cement pastes were stopped with methanol–acetone mixture (1:1). 10 g sample was pulverized in stopping mixture, and then the mixture was filtered through G_4. The solid residue was dried at 70°C for 2 h [10, 15]. The chemically combined water content of predried specimens was determined as the ignition loss 800 °C for 1 hour soaking time. Combined water content = ignition loss of the hydrated sample − (ignition loss of anhydrous mix + water of free lime) [15]. Free slag content determined according to the methods reported in earlier publication [16]. Corrections were made for neat GBFS and the loss of ignition at 800°C [17].

Thermal gravimetric analysis (TGA) was carried out using DTA-50 Thermal Analyzer (Schimadzu Co., Tokyo, Japan). A dried sample of about 50 mg (–53 µm average particle size) was used at heating rate 20°C·min^{-1} under nitrogen atmosphere. For IR spectroscopic inves-tigation, the samples were prepared using alkali halide KBr pressed disk technique. The IR analysis was recorded from KBr disks using Gensis FT-IR spectrometer in the range 400 - 4000 cm^{-1} after 256 scans at 2 cm^{-1} resolution.

The scanning electron microscope (SEM) was taken with Inspect S (FEI Company, Holland) equipped with an energy dispersive X-ray analyzer (EDX). SEM was used to examine the microstructure of the fractured composites at the accelerating voltage of 200 - 30 kV and Power zoom magnification up to 300 000×.

RESULTS AND DISCUSSION

Electrical conductivity of GBFS-MS pastes containing different contents of MS namely 0, 2, 4, and 8 mass % MS was given in Figure 4. Electrical conductivity gives an important information about the physico-chemical changes taking place during early hydration periods [10, 13, 14]. Figure 4 shows the electrical conductivity time-curve from 20 min up to 28 days. Electrical conductivity of alkaline activated GBFS-MS pastes shows a higher maximum at early ages. The increase of

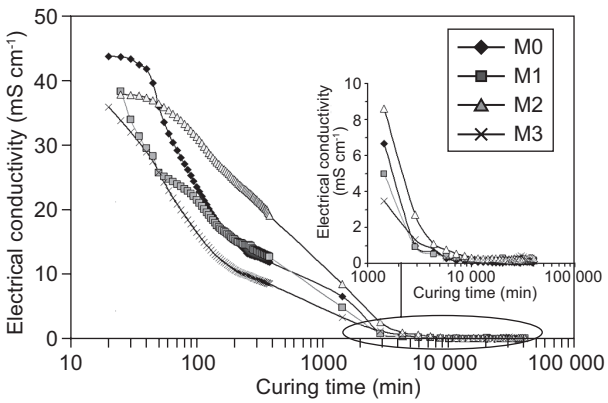

Figure 4. Electrical conductivity of alkali activated GBFS-MS as a function of curing time.

the electrical conductivity maxima at initial curing time is due to the free OH^- and Na^+ ions released from the pores of the fresh pastes. These ions act as charge carriers, leading to rapid increase in the electrical conductivity maximum. Once the concentration of these ions in the solution become very high, the ionic association starting taking place, then the concentration of these ions start to decrease after 30 min. During the induction period, some of these ions adsorbed and precipitated with the formation of amorphous C–S–H, C–A–H and C–A–S–H gel [10, 18], forming electrical double layer or protective film leading to decrease the mobility of the ions. The increase of MS content, the electrical conductivity maxima decreases; this is due to the high surface area and high pozzolanic activity of MS. The presence of 2 mass % MS the electrical conductivity peak shows a slight shift at longer hydration time, this is due to MS forms a protective film around GBFS particles during the early stage of the hydration. Increase of MS content up to 8 mass %, the electrical conductivity maxima suffer a sharp decrease during hydration periods.

The chemically combined water contents of alkali activated GBFS-MS pastes cured up to 90 days are graphically plotted as a function of curing time in Figure 5. The chemically combined water content increases gradually with curing time for all alkaline activated GBFS-MS pastes; this is due to the progress of hydration products. The chemically combined water contents of M2 mix gives the higher values at all curing ages, this is due to the formation of C–S–H, C–A–H and C–A–S–H and gehlenite-like hydrate. The increase of chemically combined water contents may be due to the higher pozzolanicity of MS up to 4 mass % MS. Whereas, the increase of the content of MS (> 4 mass %), the chemically combined water content decreases [19]. The decrease in the chemically combined water content of mix M3 is mainly due to the formation of C–S–H with lower water content than that formed from the alkali activated neat GBFS. Increase the content of MS (> 4 mass %), may form a coated film on alkali activates GBFS grains, hence the chemically combined water decreased.

The results of the combined slag contents of alkali activated GBFS-MS pastes are graphically represented in Figure 6. It is clear that the combined slag contents for all mixes increase with curing time. The combined slag content increases with curing ages up to 90 days. The combined slag content increases with the content MS up to 4 mass %. The alkaline activation GBFS is a complex process where the destruction of the GBFS structure is firstly produced and subsequently a poly-condensation – crystallization of reaction products occurs [8]. Alkaline cations play a catalytic role in the early stages of hydration involving interchange with Ca^{2+} cations. In the later stage, they combined into the structure to form zeolite-like phases [10]. The structure and composition of C–A–S–H produced in the activation of GBFS is dependent on the type of the activator. The chemically bound Ca^{2+} in C–A–S–H is replaced by Na^+, leading to the formation of a C–(N)–A–S–H inner gel [20]. MS reacts with OH^- giving C–S–H as well as Na-silicate hydrate [10]. Therefore, as the amount of MS increases the combined slag content increases. Increase of the content MS up to 8 mass % the combined slag content decreases than those of neat paste containing only GBFS up to 3 days, whereas the combined slag content increases up to 90 days. Alkali activated GBFS-MS tends to form a thin layer of products around unreacted slag grains. The thin layer formed acts as a physical barrier, slowing down the movement of ions to the GBFS grain [20].

Compressive strength of hardened alkali activated GBFS-MS mixes containing different contents of MS up to 8 mass % as a partial replacement of GBFS cured for 3, 7, 14, 28 and 90 days are represented in Figure 7. The results show that the compressive strength increases

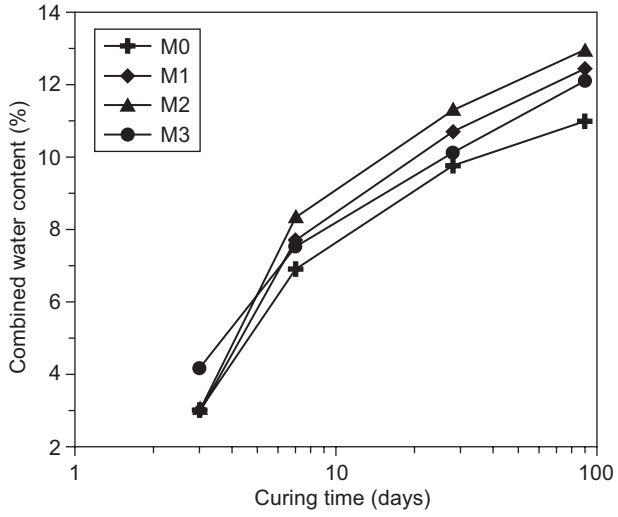

Figure 5. Chemically combined water contents of alkali activated GBFS-MS up to 90 days.

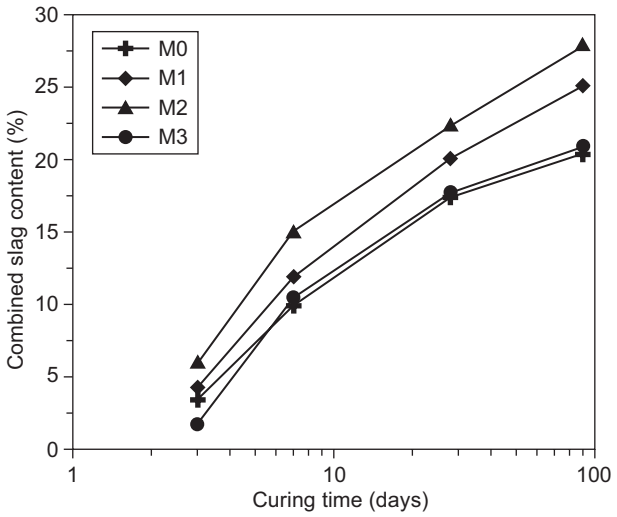

Figure 6. Combined slag contents of alkali activated GBFS-MS mixes up to 90 days.

with curing time for all hardened alkali activated GBFS-MS pastes; this is due to the progressive of hydration products, forming C–S–H as well as C–A–H and C–A–S–H gel leading to form close and compact homogeneous structure. The values of compressive strength increase with MS content up to 4 mass %. Increase in MS content up to 8 mass % the compressive strength shows a lower values at early ages (3-14 days). But, at later age up to 28-90 days, the compressive strength increases. The compressive strength values increase with 4 mass % MS, this is due to MS acts as nucleating agents or as a seeding for formation of C–S–H gel.

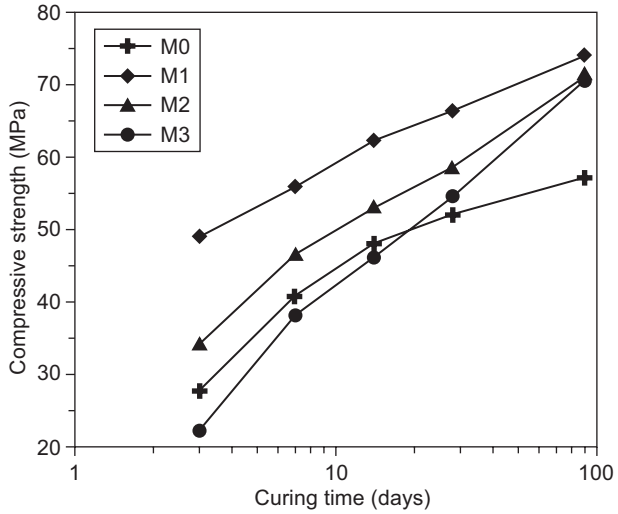

Figure 7. Compressive strength of alkaline activated GBFS-MS as a function of curing time up to 90 days.

The bulk density of alkali activated GBFS-MS mixes cured up to 90 days are graphically plotted in Figure 8. The bulk density for all hardened alkali activated GBFS-MS pastes increased with curing time, due to the continuous hydration and precipitation of the hydrated products filling up the available pore.

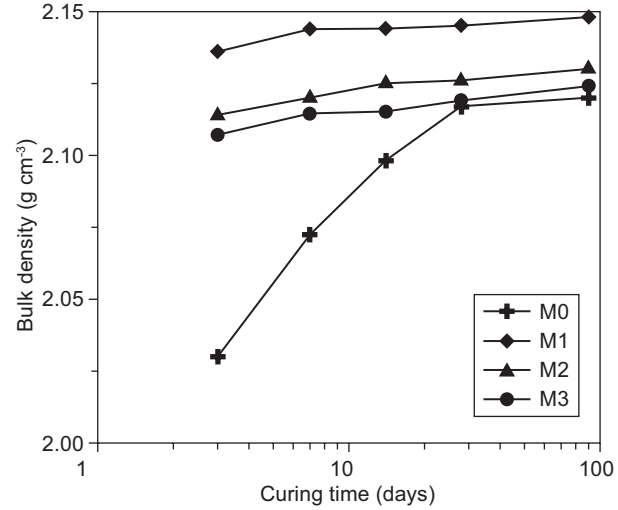

Figure 8. Bulk density of alkali activated GBFS-MS mixes as a function of curing time up to 90 days.

The bulk density of mix M0 is the lowest values while the values bulk density of mix M1 are the highest values at all curing times. MS modifies the hydrated products as well as increases the amount of calcium silicate hydrate. Alkaline activator accelerates the dissolution of Si and Al ions breaking the Si–O and Al–O bonds in GBFS-MS structure, which is followed by precipitation of low-solubility calcium silicate, calcium aluminate and magnesium aluminate hydrates to form homogeneous and denser microstructure [21].

Total porosity values of alkali activated GBFS-MS pastes are graphically plotted in Figure 9. The values of total porosity decrease till the minimum value at 90 days. Mix M0 has the higher values of total porosity. Increase the content of MS, the total porosity decreases up to 8 mass %, while mix M1 has the lowest values. Presence of MS in the alkali activated mixes cause a considerable reduction in the volume of large pores at all curing ages, MS acts as a filler due to its higher surface area [22].

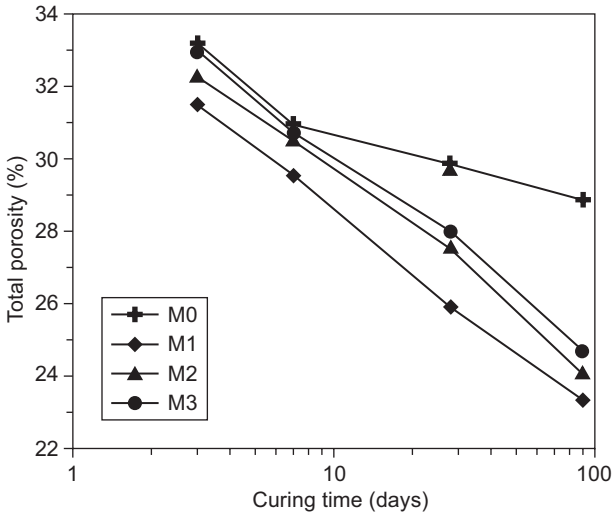

Figure 9. Total porosity of alkali activated GBFS-MS mixes as a function of curing time up to 90 days.

Figure 10 presents the thermograms of alkali activated mix M2 cured for 3, 28 and 90 days. The weight loss at 1000°C was 4.398 %, 8.861 % and 11.95 % for 3, 28 and 90 days, respectively. The weight loss observed in TGA for geopolymerized paste is attributed to the decomposition of Si–OH groups and Al–OH groups (water loss). The endothermic peak located at 60 – 90°C is due to the dehydration of free and interlayer water of C–S–H. The weight loss represented the dehydration of interlayer water of C–S–H was 2.20 %, 4.735 % and 7.97 % for mix M2 cured after 3, 28 and 90 days, respectively. The increase in weight loss is related to the progress of geopolymerization process [23]. The endothermic peak located below 200°C is related to C–A–S–H and C–A–H. The exothermic peak located at 850 – 870°C is attributed to the crystallization of the pseudo-wollastonite phase (monocalcium silicate,

CS). This exothermic peak is characteristic for the decomposition of C–S–H [24]. The endothermic peak located at 50 – 75°C is due to the dehydration of free water and C–S–H from hydrated matrix.

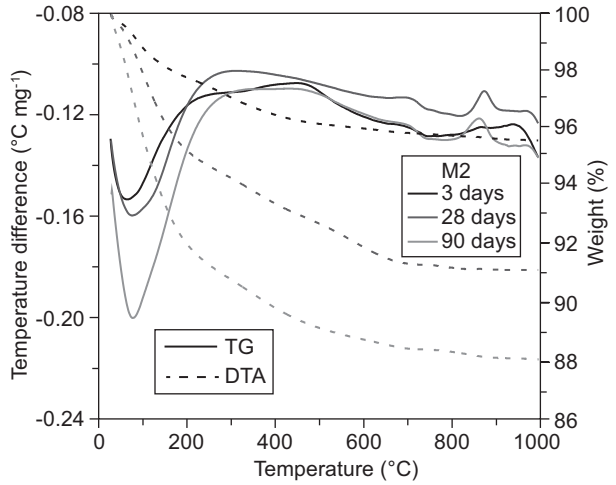

Figure 10. DTA/TG thermograms of alkali activated M2 mix cured up to 90 days.

Figure 11 presented the XRD patterns of alkali activated M2 mix containing 4 mass % MS as the partial replacement of GBFS cured up to 90 days. It can be observed that the hump peak in the range of 20 – 38° 2θ changes with curing time from 1 day to 90 days. XRD patterns illustrate the increase in calcite content. MS has higher specific surface area in interacting with dissolved calcium from GBFS forming C–S–H. MS has a positively affect on the geopolymerization process by acting as a nucleation centers for the formation and accumulation of the geopolymer [25].

FT-IR spectra of alkaline activated M2 mix are shown in Figure 12. The broad band located at 3448 and 3449 cm^{-1} are assigned to stretching vibration of H–O–H. The bending vibration frequency of H–O–H lattice in C–A–H and C–A–S–H hydrated are located at

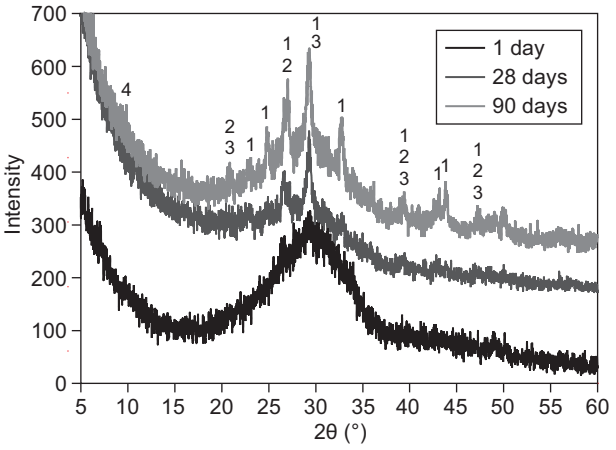

Figure 11. XRD pattrens of mix M2 activated with (0.75:0.50; Na_2O:SiO_2 mol/kg of binder) cured up to 90 days, (1= calcite; 2 = wollastonite; 3 = calcium silicate hydrate; 4 = tobromite).

1507, 1637, and 1638 cm^{-1}. The observed band at 1458, 1466, and 1489 cm^{-1} are due to the stretching vibration of C–O bond in CO_3. Its intensity decreases with curing time [26]. The band at around 1116, 1019 and 1010 cm^{-1} are due to T–O–Si (T: Si or Al) asymmetric stretching vibration as a result of TO_4 reorganization that takes place during synthesis [27]. The stretching in the region of 875 cm^{-1} is due to Si–O stretching. The bands at 477, 461 and 457 cm^{-1} are due to bending vibration of Si–O–Si and O–Si–O [25].

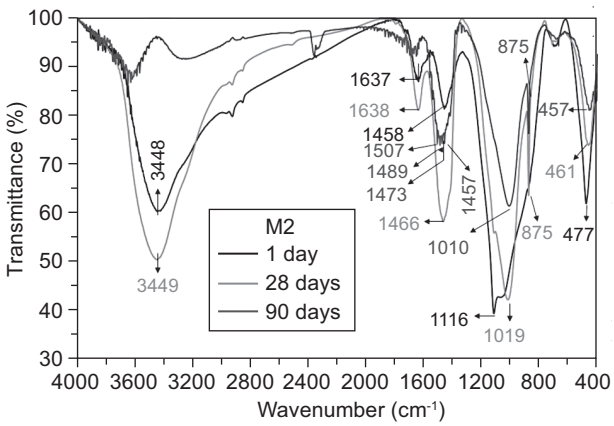

Figure 12. FTIR of mix M2 cured up to 90 days.

Figure 13 shows SEM micrographs of M0 and M2 hydrated for 3 and 90 days respectively. Figure 13a shows SEM micrograph of M0 hydrated at 3 days. Initial thin layer of hydration products formed on the surface of GBFS grains. The hydration products appeared as nearly very thin amorphous C–S–H gel covering the grains of anhydrous alkali activated GBFS particles appeared in the structure. With the increase of the hydration age up to 90 days, more hydration products observed on the surface of alkaline activated GBFS particles. C–S–H gel, C–A–H and C–A–S–H as well as flake crystal of calcium aluminate hydrates is the main hydrated products [32].

Figure 13b shows SEM micrographs of alkali activated GBFS-MS (mix M2) cured at 3 and 90 days. The micrograph of M2 mix hydrated at 3 days shows the presence of amorphous film of ill crystals of C–S–H (III) covered the surface of specimens. At 90 days, the micrograph depicts the presence of C–S–H with fibrous acicular morphology [28]. MS enhances the formation of fibrous structure of C–S–H with denser spheres [28-31], as well as forms additional nucleation or polymerization-condensation centers for the precipitation of geopolymer (N,C)ASH gel and low porosity of the developed matrix [9], as indicated from the morphology, where a massive platy geopolymer layer fill mostly the matrix composition. This compact structure of C–S–H leads to enhancement the microstructure performance providing an additional increase in compressive strength of the mix M2 containing 4 mass% MS. leads to form a denser closed microstructure, leading to higher compressive strength values.

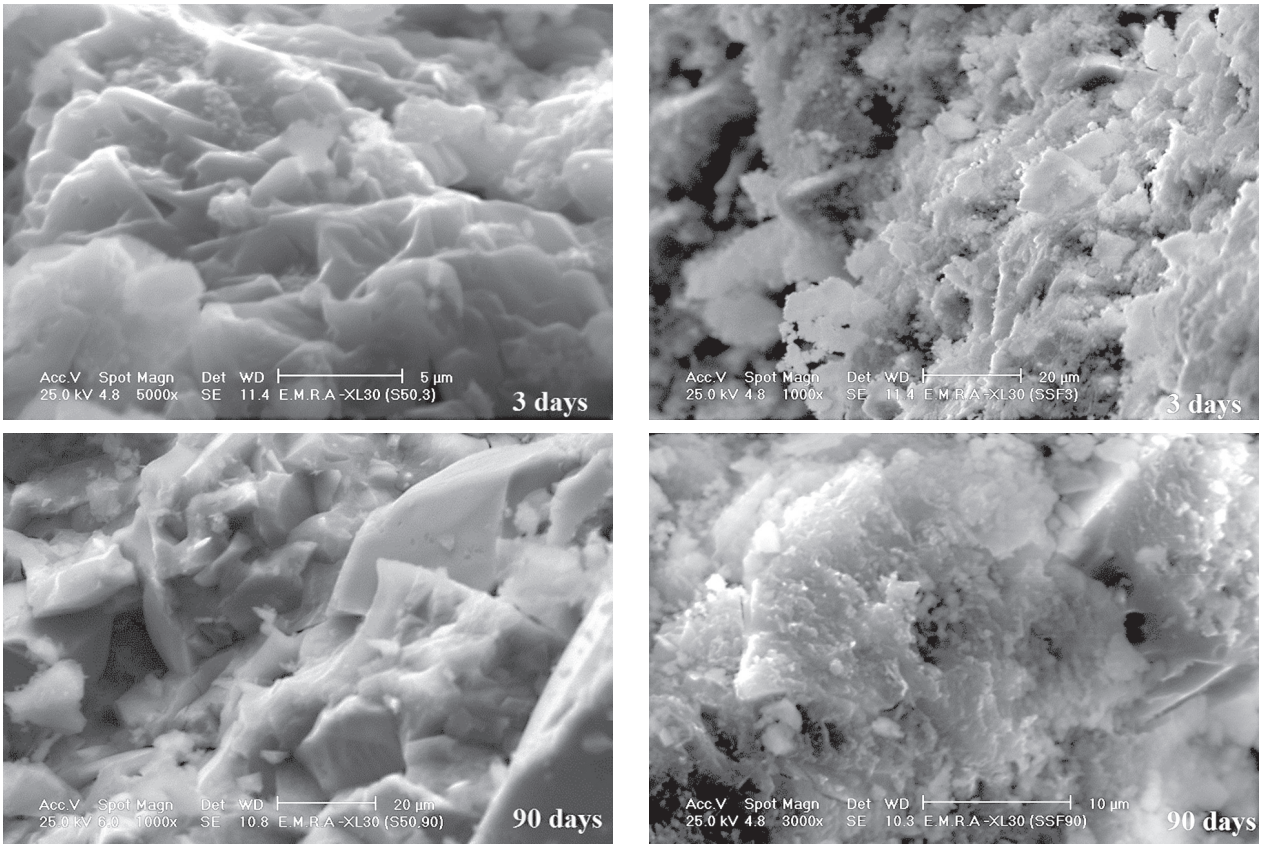

a) M0 b) M2

Figure 13. SEM micrograph of mix M0 (a) and M2 (b) cured up to 3 and 90 days.

Resistance to magnesium sulphate aggressive attack solution

When Portland cement concrete is attacked by sulphate solutions, the attack can lead to strength loss, expansion, spalling of surface layers and, ultimately, disintegration. The effects are minimized in concrete of low permeability, sulphate-resisting cement or composite cements [32]. Magnesium sulphate has a more aggressive attack solution, because $MgSO_4$ decomposes the calcium silicate hydrates during exposure to produce magnesium silicate hydrates with no binding strength and CH [15]. Chemical attack by aggressive magnesium sulphate is one of the factors responsible for damaging cement matrix [33, 34].

The compressive strength of alkali activated M0, M2 as well as OPC cement pastes immersed in 5 % $MgSO_4$ solution up to 180 days are graphically plotted in Figure 14. The compressive strength of alkaline activated GBFS increases with curing time as the hydration progresses up to 180 days. The immersion of alkali activated GBFS pastes in 5 % $MgSO_4$ solution enhances the activation of GBFS pastes [10]. The compressive strength of mix M2 shows the higher values, this is due to the higher pozzolanic activity in alkaline activation that exhibits higher resistance to sulphate medium up to 180 days. The compressive strength of alkaline activated GBFS-MS paste increases, due to the formation of additional C–S–H hydrates which deposited in the available pores and hence decreases the porosity. MS showed a good pozzolanic activity in alkaline activation to form $n_1CaO{\cdot}SiO_2{\cdot}n_2H_2O$ (C–S–H) which responsible for the higher compressive strength [35]. The compressive strength of OPC pastes immersed in 5 % $MgSO_4$ increases up to 90 days then decreases [10, 15, 36-40]. The strength of the alkali activated GBFS-MS shows higher values than those of OPC cement paste up to 180 days, due to the formation of C–S–H and geopolymer [41].

The total sulphate content of alkali activated mixes M0, M2 as well as OPC cement pastes immersed in 5 % $MgSO_4$ solution up to 180 days is represented in Figure 15. The values of total sulphate contents of alkali activated M0, M2 show a lower values up to 180 days of immersion in 5 % $MgSO_4$ solution. The resistivity towards sulphate solution increases with 4 mass % MS content, this is due to the decrease in the total porosity, which hinders the penetration of sulphate ions in the GBFS-MS paste matrix. OPC paste gives higher values of total sulphate content, whereas M2 has a lower values of total sulphate content at all curing ages, this can be attributed to the alkali activated matrixes are not easily attacked by aggressive solution, due to the absence of free lime [42].

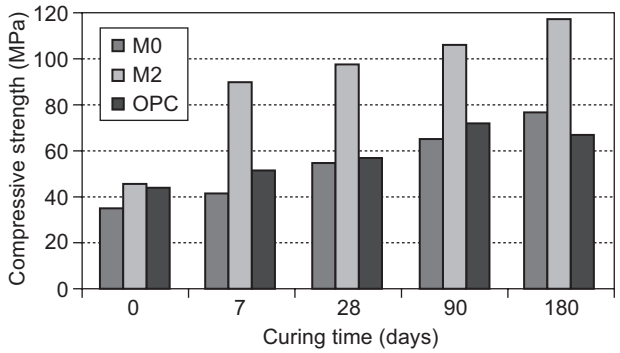

Figure 14. Compressive strength of activated GBFS-MS and OPC pastes subjected to 5 % $MgSO_4$ solution up to 180 days.

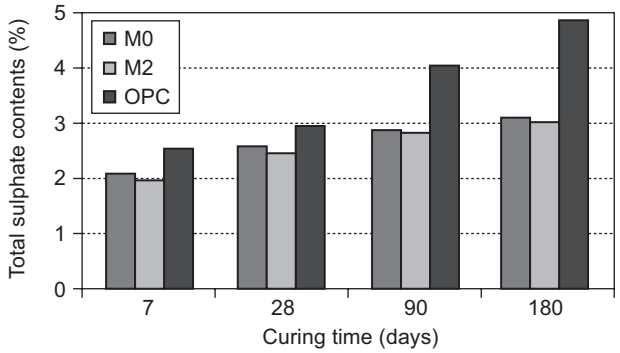

Figure 15. Total sulphate of activated GBFS-MS and OPC pastes subjected to 5 % $MgSO_4$ solution up to 180 days.

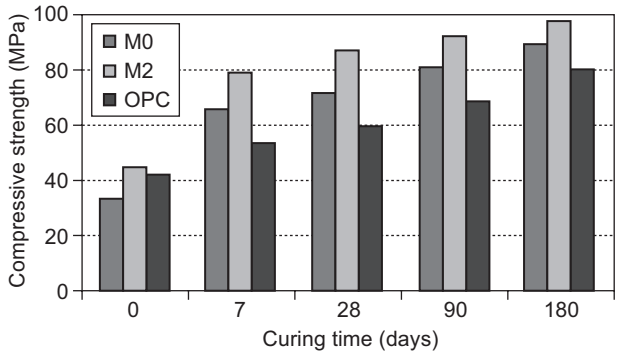

Figure 16. Compressive strength of activated GBFS-MS and OPC pastes immersed in 5 % $MgCl_2$ solution.

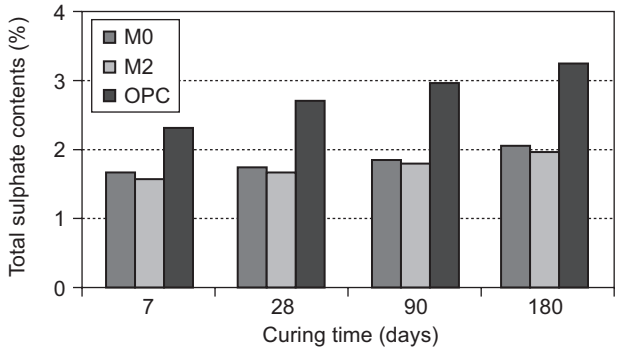

Figure 17. Total chloride of activated GBFS-MS pastes as well as OPC immersed in 5 % $MgCl_2$ solution.

Resistance to magnesium chloride aggressive attack solution:

Chloride ions are the most detrimental agents that cause quick concrete deterioration. The intensity of the corrosive action depend on the concentration of chloride solution and the kind of cation linked to the chloride ion [43]. The penetration of Cl^- ions is independent not only on the porosity of the matrix, but also on the nature of the paste and the ion-exchange capacity of the system.

The compressive strength values of alkaline activated M0, M2 as well as OPC cement pastes immersed in 5 % $MgCl_2$ solution up to 180 days are graphically represented in Figure 16. The compressive strength increases with curing time. Increase in compressive strength values is due to the promotion of hydration products as a result of the adsorption as well as incorruption of a part of Mg^{2+} ions onto the C-S-H particles which enhances the crystallization of C-S-H [15]. The values of compressive strength of OPC shows a lower values from 7 days up to 180 days. OPC contains free CH in its matrix attacked by Cl^- ions [36, 38, 44]. The compressive strength of mix M0 increases gradually up to 180 days due to good resistance to chloride medium, whereas, the values of compressive strength of OPC shows a lower values from 28 days up to 180 days [10]. Replacement 4 mass % GBFS with MS (mix M2) increases the values of compressive strength than neat GBFS mix (M2). MS has higher surface area and high pozzolanic activity values, which enhanced with the action of alkaline activator. MS decreases the total porosity, hence increases the durability of GBFS-MS binder. M2 gives the higher values of compressive strength than all investigated binders, due to the formation of a denser structure enhances the durability to chloride medium up to 180 days.

The total chloride contents of alkali activated M0, M2 as well as OPC cement pastes immersed in 5 % $MgCl_2$ solution up to 180 days are graphically plotted in Figure 17. The total chloride content increases with curing time for all mixes up to 180 days. The total chloride sharply increases after first week up to 28 days, and then it slowly increases up to 180 days for all pastes. The increase in total chloride contents of hardened OPC pastes up to 180 days is due to the reaction of $MgCl_2$ with liberated CH forming $CaCl_2$ and $Mg(OH)_2$. $CaCl_2$ reacts with C_3A and/or C_4AF to form chloroaluminate hydrate ($C_3A.CaCl_2.10H_2O$) as well as $MgCl_2$ reacts with C–S–H hydrates to form $CaCl_2$, magnesium hydroxide and silica gel. The total chloride contents of M0 and M2 mixes decrease, this is due to the pozzolanic reaction to form C–S–H that fill some available open pores forming more dense low capillary pore structure on the prolonged hydration, thereby inhibiting the chloride ion penetration; improve the microstructure of pore systems. Mix M2 shows lower values of chloride contents up to 180 days. The decrease of the Cl^- ions diffusion is attributed to the precipitation of more hydration products from the

pozzolanic activity of MS to form additional C-S-H. M0 and M2 mixes do not have free lime content in these matrixes, geopolymers and are not easily attacked by Cl^- ions [42].

CONCLUSIONS

The main conclusions could be derived from this investigation are summarized as follows:

- GBFS-MS mixes suffer a sharp decrease in electrical conductivity maxima during hydration periods. The presence of 2 mass % MS shows a slight shift in the electrical conductivity peaks to longer hydration time.
- The chemically combined water contents of mix M2 gives the higher values at all curing ages.
- The combined slag content increases with MS contents up to 4 mass %.
- Mix M1 shows the higher values of compressive strength at all curing ages. The increase in compressive strength is due to higher surface area and effective pozzolanic activity of MS, it acts as nucleating agents or as a seeding for formation of C–S–H gel.
- The compressive strength of M2 mix in sulphate and chloride aggressive solutions shows higher values up to 180 days.
- The total sulphate and chloride contents of alkali activated mix M2 shows a lower values of sulphate or chloride contents in 5 % $MgSO_4$ or 5 % $MgCl_2$ solutions.
- It can be concluded that alkali activated GBFS-MS are more durable in 5 % $MgSO_4$ or 5 % $MgCl_2$ than OPC pastes.

REFERENCES

1. Sayed M., Zeedan S.R.: HBRC *8*, 177 (2012).
2. Siddique R.: *Waste materials and by-products in concrete*, Springer-Verlag Berlin Heidelberg, p. 1-40, 2008.
3. Uchikawa H. in: Proceedings of the 8th Inter Congr. Chem. Cem. Concr., p. 249–280; Principal Report (Brazil), 1986.
4. Malhotra V.M., Ramachandran V.S., Feldman R.F., Aitcin P.C.: *Condensed silica fume in concrete*, CRC Press, Inc , Boca Raton, Florida 1987.
5. Wang S.D., Scrivener K.L.: Cem. Concr. Res. *33*, 769 (2003).
6. Glukhovsky V. in: 1st Inter. Conf. Alkaline Cements and Concretes, p. 1-8, Kiev, Ukraine, 1994.
7. Krivenko P.D. in: Paper presented Inter. Conf. on alkaline cement and concretes, Kiev, Ukarine, 1994.
8. Fernandez-Jimenez A., Puertas F., Sorbrados I., Sanz J.: J. Amer. Ceram. Soc. *86*, 1389 (2003).
9. Fernandez-Jimenez A., Puertas F.: Adv. Cement. Res. *13*, 115 (2001).
10. Heikal M., Nassar M.Y., El-Sayed G., Ibrahim S.M.: Constr. Buil. Mater. *69*, 60 (2014).
11. Juenger M.C.G., Ostertag C.P.: Concr. Sci. Eng. *4*, 91 (2002).
12. American Society for Testing and Materials, ASTM Standards, Standard Test Method for Normal consistency of Hydraulic cement, American Society for Testing and Materials, C 187-83, 195, 2008.
13. Heikal M., Aiad I., Helmy I.M.: Cem. Concr. Res. *32*, 1805 (2002).
14. Heikal M., Morsy M.S., Radwan M.M.: Cem. Concr. Res. *35*, 1438 (2005).
15. Abd-El. Aziz M.A., Heikal M.: Adv. Cem. Res. *21*, 91 (2009).
16. Heikal M., Morsy M.S., El-Shimy E., Abo-El-Enein S.A.: l'industria Italiana del Cemento (iiC) *7-8*, 614 (2004).
17. Stark J., Ludwing H.M., Müller A.: Zement Kalk Gips *90*, 557 (1991).
18. Tashima M.M., Soriano L., Borrachero M.V., Monzó J., Payá J.: Bull. Mater. Sci. *36*, 245 (2013).
19. Kar A., Ray I., Unikrishnan A., Davalos F.: Cem. Concr. Comp. *34*, 419 (2012).
20. Haha M.B., Saout G.L., Winnefeld F., Lothenbach B.: Cem. Concr. Res. *42*, 74 (2012).
21. Wu X., Jiang W., Roy D.M.: Cem. Concr. Res. *20*, 961 (1990).
22. Siddique R., Khan M.I.: *Supplementary Cementing Materials:Silica Fume, Engineering Materials, Ch:2*, p. 67-119, Springer-Verlag, Berlin Heidelberg, 2011.
23. Tashima M.M., Akasaki J.L., Castaldelli V.N., Soriano L., Monzó J., Payá J.: Mater. Lett. *80*, 50 (2012).
24. Ramachandran V.S., Paroli R.M., Beaudoin J.J., Delgado A.H.: *Handbook of Thermal Analysis off Construction Materials.* p. 692, William Andrew Publishing Norwich, New York, USA, 2002.
25. Khater H.M.: Inter. J. Adv. Structural Eng. 5 (2013).
26. Heikal M., Abd El Aleem S., Morsi W.M.: HBRC J. 9243 (2013).
27. Gadsden J.A.: *Infrared spectra of minerals and related inorganic compounds.* Butterworths, London, 1975.
28. Diamond S. in: Proceedings of the VIII Cong. Cem. Chem., p. 122–147, Rio de Janeiro, Brazil, 1986.
29. Taylor H.F.W.: *Cement chemistry*, 2nd Ed., Thomas Telford edition published, 1997.
30. Malhotra V.M., Mehta P.K.: *Pozzolanic and cementitious materials, Advances in concrete technology,* Ottawa: Overseas Publishers Association; 1996.
31. Gleize P.J.P., Müller A., Roman H.R.: Cem. Concr. Comp. *25,* 171 (2003).
32. Taylor H.F.W.: *Cement chemistry.* 2nd edition, Thomas Telford Publishing, 1997.
33. Sahmaran M., Kasap O., Duru K., Yaman I.O.: Cem. Concr. Comp. *29*, 159 (2007).
34. Al-Dulaijan S.U.: Constr. Build. Mater. *21*, 1792 (2007).
35. Wang K.S., Lin K.L., Huang Z.Q.: Cem. Concr. Res. *31*, 97 (2001).
36. El-Didamony H., Amer A.A., Abd El-Aziz H.: Ceram. Inter. *38*, 3773 (2012).
37. Abd El-Aziz M., Abd El-Aleem S., Heikal M., El-Didamony H.: Cem. Concr. Res. *35*, 1592 (2005).
38. Hime W.G., Mather B.: Cem. Concr. Res. *29*, 789 (1999).
39. Hewlett P.C.: *Lea's Chemistry of Cement and Concrete,* Butterworth-Heinemann, Technology & Engineering, p. 1092, 2003.
40. Dinakar P., Babu K.G., Santhanam M.: Cem. Concr. Comp. *30*, 880 (2008).
41. Yip C.K., Lukey G.C., Provis J.L., Van Deventer J.S.J.: Cem. Concr. Res. *38*, 554 (2008).
42. Escalante-Garcia J.I., Fuentes A.F., Gorokovsky A., Fraire-Luna P.E., Mendoza-Suarez G.: J. Am. Ceram. Soc. *86*, 2148 (2003).
43. Bensted J., Barnes P.: *Structure and Performance of Cements.* Second edition, Spon Press Taylor & Francis Group, 2008.
44. Hajimohammadi A., Provis J.L., van Deventer J.S.J.: J. Colloid Interface Sci. *357*, 384 (2011).
45. Bakharev T., Sanjayan J.G., Cheng Y.B.: Cem. Concr. Res. *33*, 1607 (2003).